

Shared Autonomy System for Turning Tracked Vehicles on Rough Terrain Using Real-Time Terrain Scanning

Yoshito Okada, Keiji Nagatani, Kazuya Yoshida^{*1}, Tomoaki Yoshida and Eiji Koyanagi^{*2}

^{*1} Department of Aerospace Engineering, Tokoku Univ.
6-6-01 Aramaki Aza Aoba, Aoba-ku, Sendai, 980-8579, Japan

^{*2} Future Robotics Technology Center, Chiba Institute of Technology
2-17-1 Tsudanuma, Narashino, Chiba, 275-0016, Japan

Abstract:

Tracked vehicles are frequently used as search-and-rescue robots for exploring areas affected by disasters. To enable good locomotion during search-and-rescue operations on rough terrain, some of those robots are equipped with active flippers. However, the manual control of such flippers requires a highly skilled operator, particularly when teleoperating with limited camera views.

To eliminate this problem, we have developed a shared autonomy system that uses a manual controller for the main tracks and an autonomous controller for the active flippers. However, this system has a limitation in that the controller spreads out the flippers to maintain contact with the ground, and thus, the autonomous flipper motions hinder the turning motion of the robot.

In this paper, we introduce a new autonomous controller for the flippers to support the turning motion of tracked vehicles. The new controller can be used instead of the previously developed controller, and it complements our shared autonomy system. We also validate the reliability of the new controller by performing experiments on an actual rough terrain.

1. INTRODUCTION

A number of research institutes are developing search-and-rescue robots for exploring disaster areas and obtaining information on victims ⁽¹⁾. These robots are expected to support rescue operations and minimize the risks of secondary injury to rescuers and victims. It is extremely important for these robots to have high mobility on the rough terrain of disaster areas that are often strewn with rubble, so tracked vehicles are frequently used ⁽²⁾⁽³⁾.

Some of tracked vehicles used for search-and-rescue operations are equipped with active flippers to enhance their traversability and stability on rough terrain (Fig. 1). Active flippers are swingable sub-tracks that negotiate steps and bumps on uneven ground. Our tracked vehicle testbed Kenaf comprises four active flippers, one located at each corner of the body covered with the two main tracks (Fig. 2). This has proven to be one of the best configurations that enables good locomotion on rough terrain, and it has won the best mobility

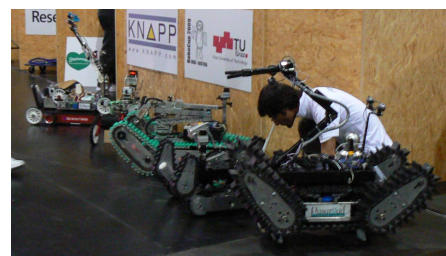


Fig. 1 Tracked vehicles with active flippers

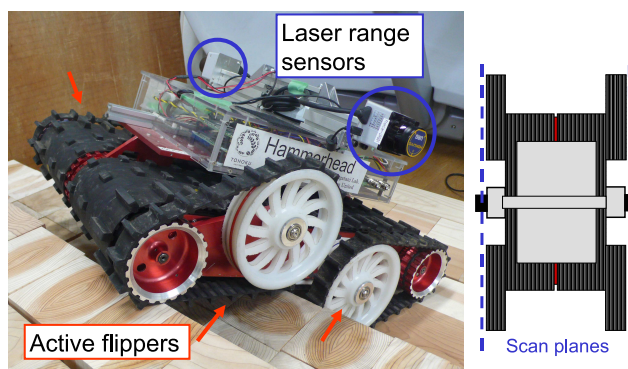


Fig. 2 Tracked vehicle testbed Kenaf

Table 1 Basic specifications of Kenaf

Dimensions	W 400 [mm] × L 500 [mm]
Weight	20 [kg]
Length of flippers	235 [mm]
Degrees of freedom	6 (2 main tracks and 4 flippers)

award twice in the RoboCup Rescue Real Robot League ⁽⁴⁾ in 2007 and 2009.

However, through such competitions and experiments, we observed that the manual control of the active flippers considerably increases the workload of the operator controlling the robot. The manual control of the robot becomes even more difficult when the operator teleoperates the robot with limited camera views.

To eliminate this problem, we have developed a shared autonomy system that uses autonomous controller for the active flippers ⁽⁵⁾. Our system generates flipper motions autonomously on the basis of real-time terrain slices along

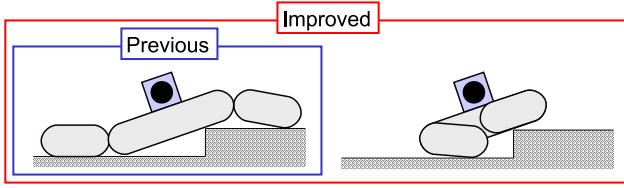


Fig. 3 Comparison between previous and new autonomous controller for flippers

the flippers obtained by two laser range sensors attached to both sides of the robot body. In a previous paper ⁽⁵⁾, we reported that our system demonstrated stable navigation on rough terrain, with the operator required only to specify the direction of travel.

Although our system with the previously developed controller is reliable when the operator directs the robot on a straight path, the previous study revealed a limitation of the controller; it spreads out the flippers to make contact with ground, so the generated flipper motions hinder the turning motion of the robot.

In this paper, we propose a new autonomous controller for flippers and introduce an improved shared autonomy system for tracked vehicles equipped with flippers. Fig. 3 shows a comparison between the previous and the new controller. The most significant difference between the two controllers is that the new one generates flipper motions within the length of the robot body to facilitate the turning motion of the robot. Similar to our previous model, the new controller ensures that the flippers make contact with the ground to maintain the stable posture of the robot body.

We incorporated the new controller for flippers into our shared autonomy system. The operator can select which autonomous controller to use, the previous or the new one, and instruct the robot accordingly. We consider that the system with the previous controller is likely to show higher stability because it makes contact with the ground to a greater extent. Therefore, the robot will show optimal performance if the operator adopts the previous controller when directing the robot on a straight path and the new one when turning or spinning it.

The rest of this paper is organized as follows. In Sec. 2, we introduce our tracked vehicle testbed Kenaf in brief. In Sec. 3, we present our strategy for the autonomous controllers of the flippers, which is based on the manual control motions of skilled operators. In Sec 4, we describe an algorithm that realizes the strategy presented in the previous section by focusing on the differences between the current and the previous algorithm for autonomous flipper control. We then report on our experiment. We incorporated the improved shared autonomy system that uses the new and the previous autonomous controls for the flippers and manual control for the main tracks into Kenaf, and performed an experiment on actual rough terrain. We present our experiment results and discuss our findings in Sec. 5. Finally, we conclude our study in Sec. 6.

2. CONTROL TARGET

We used the tracked vehicle testbed Kenaf (Fig. 2) for the purpose of improving our shared autonomy system and validating its reliability, in a similar manner to the previous study ⁽⁵⁾. Table 1 shows its basic specifications. Kenaf is a 6-D.O.F (degree of freedom) tracked vehicle testbed for rescue operations; it has four active flippers, one located at each corner of the body which is covered with two main tracks.

To obtain real-time terrain slices, two laser range sensors are attached to both sides of Kenaf's body. All the motors on Kenaf are encoder-equipped, and the circumferential velocities of the main tracks and angular positions of the flippers can be conveyed to the control unit. Moreover, Kenaf has a three-dimensional posture estimation unit comprising a 3-D.O.F gyroscope and an acceleration sensor. This unit estimates the body posture using the gyroscope, and corrects it using gravity direction from the acceleration sensor when Kenaf stops. Using the circumferential velocity of the main tracks and the body posture, we can estimate the position of Kenaf using an odometry technique ⁽⁶⁾.

3. CONTROL STRATEGY FOR FLIPPERS

In this study, our goal was to develop a system that controls the stable turning motion of the tracked vehicle by an unskilled operator with our improved shared autonomy system, including the new autonomous controller for the active flippers. In the previous controller, we applied control strategies based on flipper motions of skilled operators and confirmed the validity of these strategies. The new autonomous controller was developed on the basis of the same strategies.

In the previous paper ⁽⁵⁾, we listed the following three features of full-manual operations by skilled operators:

- To enable the robot to traverse terrain smoothly, its posture must be maintained according to the slope of the ground surface.
- To enable good locomotion, the main tracks and the flippers should be in contact with the ground as much as possible.
- When the pose of the robot is unstable, rollover should be prevented by the motion of the flippers.

Taking the three above considerations into account, we applied the following strategy for the flippers and robot body:

1. The posture of the robot body must be maintained parallel to the least-squares plane of the ground surface, and the robot body must make contact with the ground.
2. The desired posture can be realized by changing the angular positions of the flippers.
3. The desired pose (desired posture and flipper positions) must be evaluated and redefined if it is unstable.

4. CONTROL ALGORITHM FOR FLIPPERS

In this section, we describe an algorithm based on the strategy presented in Sec. 3. The algorithm for the new autonomous controller for the flippers consists of similar procedures to the previous algorithm ⁽⁵⁾. Hence, we focus on

the differences from the previous algorithm in the following subsections, and do not go into the details of any similar procedures.

4.1 SCHEMA OF NEW ALGORITHM We refactored the previous algorithm and derived the new algorithm from it. The new algorithm is divided into seven procedures and summarized as follows:

(1) Slices of the shape of the terrain along the flippers are first obtained from the two laser range sensors located at both sides of the robot body. (2) On the basis of the positions tagged with the obtained terrain slices, we convert the coordinate systems of the terrain slices and represent them in a single coordinate system. Next, (3) the desired posture of the body is determined using the terrain slices. (4) The desired positions of the flippers that achieve the required body posture are also calculated; we use a different geometric calculation from the corresponding procedure in the previous algorithm. (5) The stability of the desired posture and flipper positions is evaluated. If the stability is not enough, (6) the desired pose is redefined and procedures (4)-(5) are repeated. Finally, when the desired flipper positions that realize a stable posture are generated, (7) the position control of the flippers is performed.

4.2 COORDINATE SYSTEMS We adopt the right-handed coordinate system. Let the origin of the robot coordinate system be the center of the robot, and its x-axis and z-axis be orthogonal to the front and top faces, respectively.

The relation between the global and robot coordinate systems represents the position and posture of the robot. In this study, we also adopt the quaternion representation to describe positions and postures. For example, let the quaternion p denote the position vector $(x_{pos}, y_{pos}, z_{pos})^T$ in the global system and the quaternion q denote the θ_{rot} -rotation about the axis of the unit vector $(x_{rot}, y_{rot}, z_{rot})^T$. The coordinate conversion from a local system p, q to the global system can then be described by the following equation:

$$p_{global} = q \times p_{local} \times q^{-1} + p \quad (1)$$

$$p = [0, x_{pos}, y_{pos}, z_{pos}]^T \quad (2)$$

$$q = [\cos(\theta_{rot}/2), x_{rot} \sin(\theta_{rot}/2), y_{rot} \sin(\theta_{rot}/2), z_{rot} \sin(\theta_{rot}/2)]^T \quad (3)$$

4.3 GROUND DETECTION At the beginning of the new algorithm, the scanned points U in the robot coordinate system at the moment of scanning are detected by a laser range sensor on the robot. We tag U with the estimated position quaternion p and posture quaternion q in the global system at the moment of scanning, and define them as the two-dimensional terrain information $S = \{U, p, q\}$.

For each control loop, we use the combination of scanned points from the right and left laser range sensors as in the following equation:

$$S_n = \{S_{l,n}, S_{r,n}\} \quad (4)$$

where subscripts l and r denote the terrain slices from the

left and right sensors, respectively, and subscript n indicates a terrain slice obtained during the n th control loop.

4.4 INTEGRATION OF TERRAIN SLICES We then integrate the scanned points in S_n and select the ones to be targeted in the following procedures. If the desired robot pose determined in a following procedure is realized by Δt later, the robot position p' after Δt can be described by the following equation:

$$p' = p_{cur} + q_{cur} \times [0, V_{cur} \Delta t, 0, 0]^T \times q_{cur}^{-1} \quad (5)$$

where V is the translational velocity of the robot and the subscript 'cur' denotes a current value. We trim the scanned points in S_n based on p' through the following steps; the coordinate conversion of a scanned point u from the tagged system $\{p, q\}$ to the robot system $\{p', q_{cur}\}$ after Δt , is described by the following equation:

$$u' = q_{cur}^{-1} \times (q \times u \times q^{-1} + p - p') \times q_{cur} \quad (6)$$

We apply this conversion to each $S = \{U, p, q\} \in S_n$ and integrate the converted points to generate the three-dimensional terrain information U'_n , in which all the scanned points are represented in the same coordinate system.

We then select the target points U_{target} out of U'_n for the following procedures, according to the following equation:

$$U_{target} = \{u \in U'_n \mid -L/2 \leq x \leq L/2 \text{ and } -W/2 \leq y \leq W/2\} \quad (7)$$

where L is the entire length of the robot with the flippers, and W is the width of the robot.

4.5 DETERMINATION OF DESIRED POSTURE As mentioned previously, for the control strategy of the new controller, the desired posture of the robot body is initialized to be parallel to the least-squares plane of the ground surface and in contact with the ground. We first calculate the quaternion q_{target} which represents the parallel posture of the least-squares plane of U_{target} determined in the last subsection. U_{target} is then converted to the robot system for the case where the posture of the robot is equal to q_{target} ; let this be U'_{target} . Finally, we convert U'_{target} to the robot system for the case where the robot makes contact with the ground; let this be U''_{target} . The above conversions are summarized in the following equations using $u \in U_{target}, u' \in U'_{target}$ and $u'' \in U''_{target}$:

$$u' = q_{target} \times u \times q_{target}^{-1} \quad (8)$$

$$u'' = u' - [0, 0, 0, \max(z' \in U'_{target})]^T \quad (9)$$

To realize control strategy 1, we assume the converted terrain information U''_{target} as the target for the following procedures.

4.6 DETERMINATION OF DESIRED FLIPPER POSITIONS In this procedure, using the desired body posture and the integrated terrain slices, we determine the desired flipper positions based on a geometric calculation.

In the improved shared autonomy system, the operator can select which calculation method is used to determine the desired flipper positions - the previous method or the new

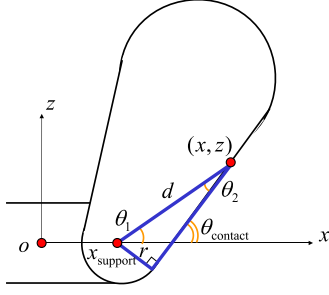


Fig. 4 Contact with straight section (spreading mode)

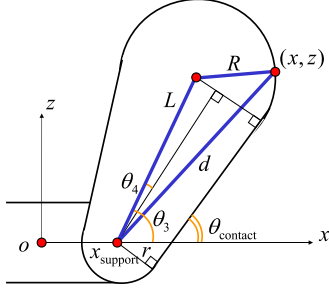


Fig. 5 Contact with round section (spreading mode)

one. We call the previous method the Spreading mode and the new one the Folding mode.

In both modes, to realize control strategy 2, we determine the desired flipper positions to make contact with the ground surface in the desired robot posture. In particular, we calculate the angular position of each flipper that makes contact with each scanned point along the length of the flipper. The desired position of each flipper is determined for the maximum or minimum angular position of the flipper in the spreading or folding mode, respectively.

Because the flippers are tracked, they comprise of a straight section and a round section. Hence, we should distinguish which part of the flipper each scanned point makes contact with by the distance between the supporting point of the flipper and the contact point, and adopt the appropriate geometric calculation. The threshold $d_{threshold}$ equals the distance to the boundary point between the straight and round sections. When the distance d to the point is less than $d_{threshold}$, the flipper will make contact with its straight section. If it is greater, the flipper will make contact with its round section.

4.6.1 SPREADING MODE When the spreading mode is adopted by the operator, the desired flipper positions are determined in the same way that was used in the previous controller.

Fig. 4 shows a flipper that makes contact with the straight section. The contact angular position of the flipper is described by the following equation:

$$\begin{aligned} \theta_{contact} &= \theta_1 + \theta_2 \\ &= \tan^{-1} \frac{z}{x - x_{support}} \\ &\quad + \sin^{-1} \frac{r}{\sqrt{(x - x_{support})^2 + z^2}} \end{aligned} \quad (10)$$

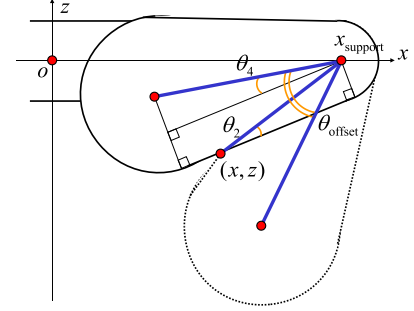


Fig. 6 Contact with straight section (folding mode)

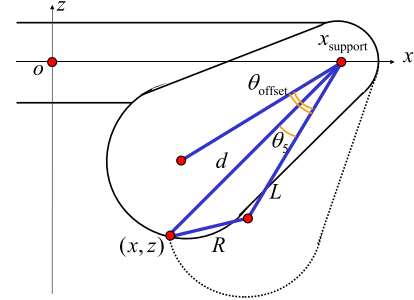


Fig. 7 Contact with round section (folding mode)

Fig. 5 shows a flipper in a contact with the round section. The contact angular position is described by the following equation:

$$\begin{aligned} \theta_{contact} &= \theta_3 - \theta_4 \\ &= \cos^{-1} \frac{d^2 + L^2 - R^2}{2Ld} + \tan^{-1} \frac{z}{x - x_{support}} \\ &\quad - \sin^{-1} \frac{R - r}{L} \end{aligned} \quad (11)$$

Each desired flipper position for the contactable points $\{u_1, u_2, \dots, u_n\}$ is determined by the following equation:

$$\theta_{ref} = \max(\theta_{contact,1}, \dots, \theta_{contact,n}) \quad (12)$$

4.6.2 FOLDING MODE When the folding mode is adopted by the operator, the desired flipper positions are calculated according to the following method.

Fig. 6 shows a flipper that makes contact with the straight section in the folding situation. The contact angular position can be derived from the equations of the spreading situation as follows:

$$\begin{aligned} \theta_{contact} &= (\theta_1 + \theta_2) - \theta_{offset} \\ &= (\theta_1 + \theta_2) - 2(\theta_2 + \theta_4) \\ &= \tan^{-1} \frac{z}{x - x_{support}} \\ &\quad - \sin^{-1} \frac{r}{\sqrt{(x - x_{support})^2 + z^2}} \\ &\quad - 2 \sin^{-1} \frac{R - r}{L} \end{aligned} \quad (13)$$

Fig. 7 shows a flipper that makes contact with the round section in the folding situation. The contact angular position

here can also be described based on the spreading situation equations, as follows:

$$\begin{aligned}
\theta_{contact} &= (\theta_3 - \theta_4) - \theta_{offset} \\
&= (\theta_3 - \theta_4) - 2\theta_5 \\
&= \tan^{-1} \frac{z}{x - x_{support}} \\
&\quad - \sin^{-1} \frac{R-r}{L} - \cos^{-1} \frac{d^2 + L^2 - R^2}{2Ld} \quad (14)
\end{aligned}$$

Each desired flipper position for the contactable points $\{u_1, u_2, \dots, u_n\}$ is determined by the following equation:

$$\theta_{ref} = \min(\theta_{contact,1}, \dots, \theta_{contact,n}) \quad (15)$$

4.7 STABILITY EVALUATION OF DESIRED POSE

Through the above procedures, we have obtained the desired pose that denotes the desired posture of the robot body and flipper positions. In this procedure, we evaluate the stability of the desired pose, as required by the control strategy 3. We have adopted the normalized energy stability margin (NESM) proposed by Hirose et al. ⁽⁷⁾ as the stability criterion as well as the previous algorithm.

The NESM is determined by the vertical distance between the initial position of the center of gravity and its highest position when rotating around an axis which runs through two contact points between the robot and the ground. Although its calculation requires the positions of the contact points, we can alternatively obtain them through the desired flipper positions. For tracked vehicles with four flippers, we can assume four rotating axes that pass through the following pairs of contact points: the front right and front left, front right and rear right, front left and rear left, and rear right and rear left. The stability of the robot is determined by the minimum value of NESM about these four axes.

4.8 REDEFINITION OF DESIRED POSE

When the stability of the desired pose is less than a predetermined threshold, we redefine the desired posture and flipper positions as well as the previous algorithm according to control strategy 3. We divide this procedure into the following steps:

- 1a. When the NESM about the front or rear is adopted, reduce the pitch angle of the desired posture to close to zero.
- 1b. When the NESM about the right or left is adopted, reduce the roll angle of the desired posture to close to zero.
2. Redefine the desired flipper positions by recalculating them to realize the redefined desired posture.
3. Evaluate the NESM about the redefined posture and flipper positions.

The above routine is repeated until a desired stable pose is generated.

4.9 POSITION CONTROL OF FLIPPERS

To achieve a desired stable posture of the robot body determined through the above procedures, we finally perform the position control of the flippers using a conventional PID controller. In addition, to realize the desired angular

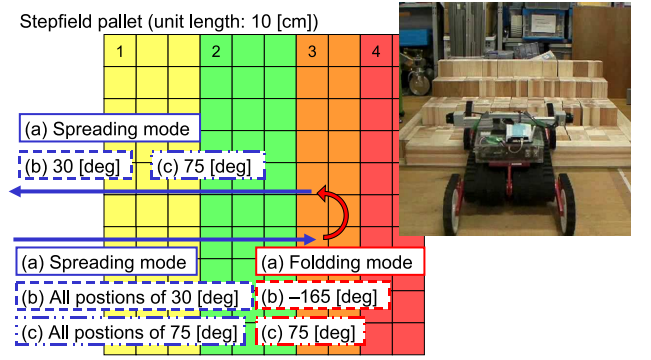


Fig. 8 Comparative experiment on stepfield pallet

positions of the flippers θ_{ref} by using Δt assumed in subsection 4.4, we can determine the maximum angular velocity of each flippers ω_{max} using the following equation:

$$\omega_{max} = C \frac{|\theta_{cur} - \theta_{ref}|}{\Delta t} \quad (16)$$

where θ_{cur} is the current angular position of the flipper and C is a given constant of proportionality.

5. EXPERIMENT

5.1 OVERVIEW We incorporated the improved shared autonomy system, comprising the manual controller for the main tracks and the autonomous controller for the flippers described in Sec. 4, into our tracked vehicle testbed Kenaf.

To validate the improved system, we performed a comparative experiment on a rough field standardized as stepfield pallets ⁽⁸⁾. The stepfield pallets are a repeatable terrain designed to evaluate the mobility of a search-and-rescue robot, formulated by NIST/ASTM. We set up a medium-size stepfield pallet in the configuration shown in Fig. 8, as our experimental field.

For the experiment, we adopted two comparative cases with static flipper positions of 75[deg] and flipper motions appropriate for the pallet, as prescribed by an expert operator. We obtained the changes in the robot posture for each trial using its built-in 3-D.O.F gyroscope.

We assumed that the time delay Δt until the desired pose is achieved to be 0.5[sec], the threshold of the stability to be 20[%] of that on level ground, and the given constant of proportionality C for the maximum angular velocity of the flippers to be 1.3. The cycle of the flipper control is 100[ms] and is dependent on the cycle of the terrain scanning by the laser range sensors.

5.2 RESULTS AND DISCUSSION In both trials with the autonomous controller for the flippers and specialized flipper motions, the robot maintained a stable posture and did not overturn. On the other hand, in the trial with the static flipper positions, the robot was stuck in the second division of the path and did not turn because of ineffective flipper positions. These results clearly show the advantage of using the flippers on rough terrain.

Figs. 9-11 and Figs. 12-14 show the changes in the pitch and roll angle, respectively, of the robot body during the

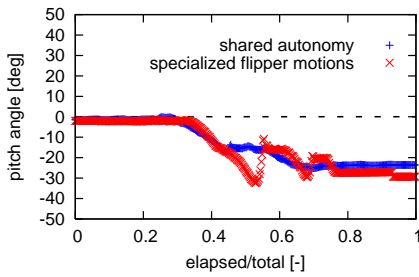


Fig. 9 Pitch angles on division 1

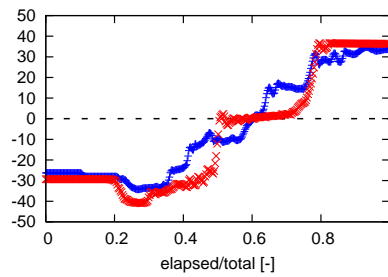


Fig. 10 Division 2

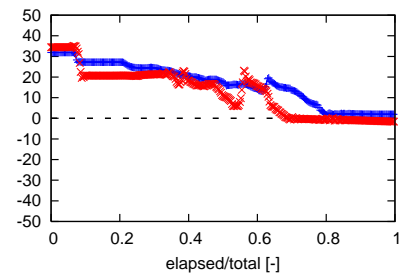


Fig. 11 Division 3

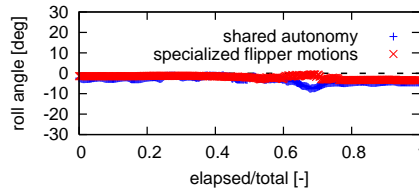


Fig. 12 Roll angles on division 1

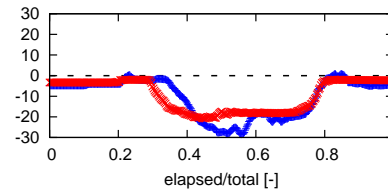


Fig. 13 Division 2

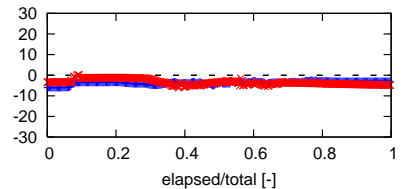


Fig. 14 Division 3

trials. For comparison, the horizontal axes in these graphs indicate the ratios obtained by dividing the elapsed time by the total time required in each division. The graphs indicate that the posture with the improved autonomous controller and the appropriate specialized flipper motions were quite similar. Thus, we confirmed that the control algorithm generated stable motions of the robot body and it is comparable an expert operator according to the control strategy.

6. CONCLUSIONS

In this study, we aimed to improve our shared autonomy system for tracked vehicles with active flippers and incorporated a new autonomous controller for the flippers to enable the robot to turn on rough terrain; our improved system comprises to a manual controller for the main tracks and two autonomous controllers for the flippers to traverse and turn. The flipper controllers employ real-time terrain scanning using two laser range sensors attached to both sides of the robot. The ground slices obtained along the flippers are integrated and used by one of the flipper controllers selected by the operator. The flipper controllers employ the same control strategy derived from flipper motions as that employed by an expert operator. These controllers generate flipper motions that control the posture of the robot body according to the average attitude above the latest obtained ground slices until the robot has attained enough stability on the rough terrain.

We performed experiments on a repeatable rough terrain using a tracked vehicle testbed with our improved shared autonomy system. The results indicated that our system enabled stable and smooth locomotion comparable to that obtained using full manual operation, including the manual control of the flippers by an expert operator, with the operator required only to specify the desired direction to the robot.

Acknowledgment

This work was supported by Strategic Advanced Robot Technology, an R&D project of NEDO, Japan.

References

- (1) S. Tadokoro, F. Matsuno and A. Jacoff, "Special Issues on Rescue Robotics," *Advanced Robotics* Vol.19 No.3, No.8, 2005
- (2) M. Guarnieri, P. Debenest, T. Inoh, K. Takita, H. Masuda, R. Kurazume, E. Fukushima and S. Hirose, "HELIOS Carrier: Tail-like Mechanism and Control Algorithm for Stable Motion in Unknown Environments," *The IEEE International Conference on Robotics and Automation*, 2009
- (3) H. Miyanaka, N. Wada, T. Kamegawa, N. Sato, S. Tsukui, H. Igarashi and F. Matsuno, "Development of a Unit Type Robot 'KOHGA2' with Stuck Avoidance Ability," *The IEEE International Conference on Robotics and Automation*, pp. 3877–3882, 2007
- (4) A. Jacoff, E. Messina, B.A. Weiss, S. Tadokoro and Y. Nakagawa, "Test Arenas and Performance Metrics for Urban Search and Rescue Robots," *The IEEE/RSJ International Conference on Intelligent Robots and Systems*, pp. 3396–3403, 2003
- (5) Y. Okada, K. Nagatani and K. Yoshida, "Semi-Autonomous Operation of Tracked Vehicles on Rough Terrain using Autonomous Control of Active Flippers," *The IEEE/RSJ International Conference on Intelligent Robots and Systems*, 2009
- (6) K. Nagatani, N. Tokunaga, Y. Okada and K. Yoshida, "Continuous Acquisition of Three-Dimensional Environment Information for Tracked Vehicles on Uneven Terrain," *The IEEE International Workshop on Safety, Security, and Rescue Robotics*, pp.25–30, 2008
- (7) S. Hirose, H. Tsukagoshi and K. Yoneda, "Normalized Energy Stability Margin: Generalized Stability Criterion for Walking Vehicles," *The International Conference on Climbing and Walking Robots*, pp.71–76, 1998
- (8) A. Jacoff, A. Downs, A. Virts and E. Messina, "Stepfield Pallets: Repeatable Terrain for Evaluating Robot Mobility," *The 8th Workshop on Performance Metrics for Intelligent Systems*, pp.29–34, 2008